Carbonates Evaporites (2019) 34:1265–1279
DOI 10.1007/s13146-017-0395-9

ORIGINAL ARTICLE

Trace and rare earth element geochemistry of Holocene hydromagnesite from Dujiali Lake, central Qinghai–Tibetan Plateau, China

Yongjie Lin[1,2] · Mianping Zheng[1,2] · Chuanyong Ye[2] · Ian M. Power[3]

Accepted: 27 August 2017 / Published online: 14 September 2017

Abstract The genesis of hydromagnesite [$Mg_5(CO_3)_4(OH)_2{\cdot}4H_2O$] has attracted great interest as a pathway for sequestering anthropogenic CO_2 and because of its importance to Mg carbonate depositional environments; however, there remain uncertainties regarding the chemical environment for hydromagnesite precipitation in modern and ancient geologic systems. Trace and rare earth element (REE) concentrations in hydromagnesite from Dujiali Lake, central Qinghai–Tibetan Plateau, China identified the formation conditions in the context of the depositional environment. The analyzed hydromagnesite samples had low total REE concentrations, varying from 0.62 to 3.11 ppm, with an average $\sum$REE value of 1.75 ppm. Comparisons of Ce/Ce* with La_N/Sm_N, Dy_N/Sm_N, and $\sum$REE showed no correlation indicating preservation of the original redox conditions during hydromagnesite precipitation. Redox-sensitive trace element ratios (U/Th, Ni/Co, V/Cr and V/V + Ni), negative Mn* values, and low authigenic uranium (U_a) values all indicate oxic conditions at the time of hydromagnesite formation. Furthermore, the Post-Archean Australian Shale-normalized REE patterns of the hydromagnesite display slight heavy REE enrichment, a slightly negative Ce anomaly, and a consistently positive Eu anomaly, which are consistent with precipitation in a predominantly oxidizing environment. Data indicate that hydromagnesite precipitated from waters influenced by both Mg-rich hydrothermal fluids and meteoric water with a similar composition to the lake water. This study provides new insights into the conditions of hydromagnesite formation at Dujiali Lake with implications for the understanding of the genesis of modern and ancient Mg carbonate deposits.

Keywords Trace element · Rare earth element · Hydromagnesite · Formation conditions · Alkaline lake · Qinghai–Tibetan Plateau

✉ Mianping Zheng
zhengmp2010@126.com

✉ Chuanyong Ye
yechuanyong@cags.ac.cn

Yongjie Lin
linyongjie2014@163.com

Ian M. Power
ianpower@trentu.ca

[1] School of Earth Sciences and Resources, China University of Geosciences, Beijing 100083, China

[2] MLR Key Laboratory of Saline Lake Resources and Environments, Institute of Mineral Resource, Chinese Academy of Geological Sciences (CAGS), NO.26, Baiwanzhuang Street, Beijing 100037, China

[3] Trent School of the Environment, Trent University, 1600 West Bank Drive, Peterborough, ON K9L 0G2, Canada

Introduction

Hydromagnesite [$Mg_5(CO_3)_4(OH)_2{\cdot}4H_2O$] is a rare magnesium carbonate mineral that was named in 1827 by Hans Gabriel Trolle-Wachmeister in reference to its composition (Trolle-Wachmeister 1827). This mineral has been reported in numerous localities in a variety of settings including lacustrine evaporites (Zheng et al. 1989; Zheng 1997; Lin et al. 2017), carbonated microbial mats and stromatolites (Renaut and Long 1989; Braithwaite and Zedef 1994, 1996; Power et al. 2007, 2009; Kaźmierczak et al. 2009; Cangemi et al. 2016), cave deposits (Fischbeck and Müller 1971; Hill and Forti 1997; Canaveras et al. 1999; Northup et al. 2001), and is commonly associated with the

weathering of ultramafic rock (O'Neil and Barnes 1971; Zedef et al. 2000; Green and Young 2006; Akhtar et al. 2009; Power et al. 2014; Wilson et al. 2009, 2014; Oskierski et al. 2013, 2016). Although extensive research has been conducted on hydromagnesite, most of these works have dealt with either its thermal decomposition (Yutaka et al. 1978; Rao and Chohan 1995; Hollingbery and Hull 2010), use as a flame retardant or fire retardant additive for polymers (Haurie et al. 2005, 2006; Hollingbery and Hull 2010; Realinho et al. 2014), or the precipitation mechanisms (Janet et al. 2007; Bonales et al. 2013). Only a small number of investigations have focused on the chemical environment and formation conditions of hydromagnesite within the depositional setting of an alkaline lake (Müller et al. 1972; Yan and Xia 1987).

Trace and rare earth elements (REE) in chemical sediments have been effectively used to elucidate palaeo-redox conditions (Liu et al. 1988; German and Elderfield 1990; Cullers 2002; Frimmel 2009; Zhao et al. 2009; Kamber et al. 2014), and the fluids from which the mineral formed (Wright et al. 1987; Frimmel 2009; Wang et al. 2014, 2015). Anomalies in concentrations of redox-sensitive elements, such as Ce and Eu, provide information on the redox state of sedimentary environments. For example, no fractionation of Ce occurs under reducing conditions, which results in minerals having enriched Ce concentrations when formed in anoxic environments (Webb and Kamber 2000; Frimmel 2009). The REE characteristics of hydrothermal carbonate deposits and marine carbonates have been extensively documented (Ekambaram et al. 1986; Bau and Möller 1992; Hecht et al. 1999; Barrat et al. 2000; Himmler et al. 2010; Loope et al. 2013; Li and Jones 2014; Wang et al. 2014; Franchi et al. 2015; Debruyne et al. 2016). Their REE concentrations, shale-normalized REE patterns, and Ce and Eu anomalies provide crucial information about the redox conditions (Sverjensky 1984; Sarkar et al. 2003; Frimmel 2009). Conversely, geochemical properties of lacustrine carbonates have received limited attention regarding their REE patterns with few datasets being reported (Yi et al. 2008; Barrat et al. 2000), particularly for magnesium carbonate minerals. Zedef and Russell (2016) provided a preliminary examination of some selected rare earth elements of hydromagnesite from Salda Gölü, Turkey. Variable contents of trace elements, total REE, and Ce anomalies in these lacustrine carbonates have provided valuable insights into the complex chemical conditions from which they formed.

Here, we report on the trace and rare earth element geochemical characteristics of Holocene hydromagnesite from Dujiali Lake, central Qinghai–Tibetan Plateau. To our knowledge, this study is the first comprehensive examination of trace and rare earth element geochemistry of hydromagnesite. Our study represents a novel use of REE distribution patterns, Ce and Eu anomalies, and selected redox-sensitive trace elements to decipher formation conditions of lacustrine carbonate. We advance the understanding of these geochemical tools for the reconstruction of lacustrine carbonates and paleo-lake environments as well as providing new insights into the formation conditions for hydromagnesite precipitation with implications for the understanding of the genesis of Mg carbonate deposits.

Site description

Tectonics and stratigraphy

Dujiali Lake is located in the central Qinghai–Tibetan Plateau, China (Fig. 1; 32°05′20″N, 88°42′10″E, 4524 m above sea level). The Dujiali Lake sub-basin was part of the ancient Selin Co basin. The Selin Co Lake gradually narrowed since the Middle Pleistocene, and divided into several small lake basins due to the local uplift caused by the tectonic movement. The multi-step lake terraces of this sub-basin are covered by Quaternary sediments that are a heterogeneous mixture of gravel, sand, silt and clay as well as salt deposits. Deeper lake sediments are mainly composed of mirabilite ($Na_2SO_4 \cdot 10H_2O$) and borax [$Na_2B_4O_5(OH)_4 \cdot 8H_2O$], while shallow sediments are covered by silt (Zheng et al. 2002). Dujiali Lake is located on the southern margin in the middle of the Bangong–Shuanghu–Changning–Menglian suture system, central Qinghai–Tibetan Plateau, and within the middle of the Bangong–Nujiang ophiolite mélange zone (Fig. 1; Pan et al. 2012). The ophiolites within the Bangong–Nujiang ophiolite mélange zone are composed mainly of MORB-type and supra-subduction zone (SSZ)-type ophiolites (Shi et al. 2005; Shi 2007).

Stratigraphically, the investigated area (Fig. 1) comprises four major lithologic groups: Niubao, Jinzhushan, Qushenla and Jiega. The Niubao group is widely distributed around the Dujiali Lake and consists of mudstones, sandstones and conglomerates. The Jinzhushan group is exposed to around the Niubao group within a small range, and this group is made up of thickly bedded conglomerates and sandstones. The Qushenla group is exposed in the northwest of the Dujiali Lake and consists of tuffaceous sandstone and andesite. The Jiega group is exposed to the southeast and southwest of the Dujiali Lake within a small range, and is made up of limestone with orbitolina and shale.

Hydrological condition

Dujiali Lake is found in a semi-closed endorheic basin that is recharged by meteoric and ground waters as well as a seasonal stream that intermittently supplies water to the

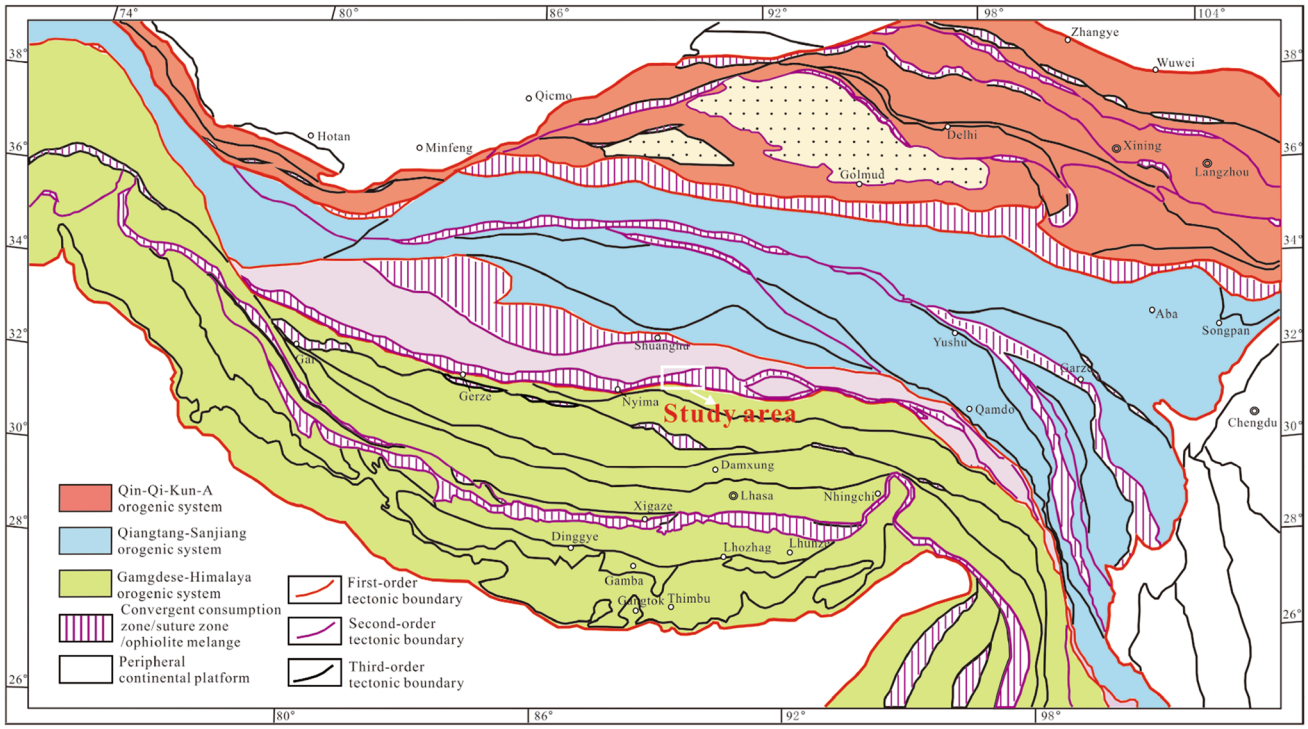

Fig. 1 Geologic map showing the tectonic units of the Qinghai–Tibet Plateau and its adjacent regions (modified from Pan et al. 2012). Note: the study area is located within the Banggong–Nujiang suture zone

southwest part of the lake. The climate in this region is classified as cold continental, sub-humid to semi-arid, with low mean annual precipitation (~200 mm) and high mean potential evaporation (~2400 mm; Zheng et al. 2002). In the 1950s, Dujiali Lake was a playa with no permanent surface water. Playa near-surface brines had salinities of ~114 g/L and average pH of 8.8 while the intercrystalline brine had a salinity of ~126 g/l (Zheng et al. 2002). An increase in precipitation and glacial meltwater due to climate change over the past decades caused the playa environment to evolve into a shallow saltwater lake. Presently, the lake has an average depth of approximately 3 m and a surface area of ~80 km^2. In our previous study (Lin et al. 2017), lake water was mildly alkaline with pH values ranging from 8.8 to 9.7. The concentration of total dissolved solids in the surface water was 1.5–9.3 g/l with Na^+, K^+, Mg^{2+}, SO_4^{2-}, HCO_3^-, CO_3^{2-}, and $B_4O_7^{2-}$ being the dominant ions.

Materials and methods

Sample description and collection

Deposits of hydromagnesite were found in the first lake terrace of the northwest of Dujiali Lake in March 2015 (see Fig. 2a, b for outcrop location). The hydromagnesite sediments directly overlay Quaternary sediments (Fig. 2c). The terrace was subparallel to the land surface and 10 m thick. Seven samples from profile DPSP01 were equidistantly collected from different horizons after removing the weathered surface crust and numbered 01 (bottom) to 07 (top). The hydromagnesite sediments were bright-white, dry, and clay-like when sampled. There were no obvious laminations or bedding in the sediments.

X-ray diffraction

Rock samples were disaggregated against a 200-mesh sieve, smear mounted onto petrographic slides with anhydrous ethanol, and allowed to dry at room temperature. X-ray diffraction (XRD) was conducted at the Key Laboratory of Saline Lake Resources and Environment, Ministry of Land and Resources, using a Rigaku MiniFlex 600 X-ray diffractometer. The long fine-focus Cu X-ray tube was operated at 40 kV and 15 mA using a take-off angle of 6°. Data were collected from 3° to 70° 2θ using a step size of 0.02°. The major crystalline mineral phases were identified with reference to the International Centre for Diffraction Data (ICDD) database using Jade data analysis program.

Major element analyses

Major element compositions were determined using X-ray fluorescence spectrometry (XRF) at the Beijing Research

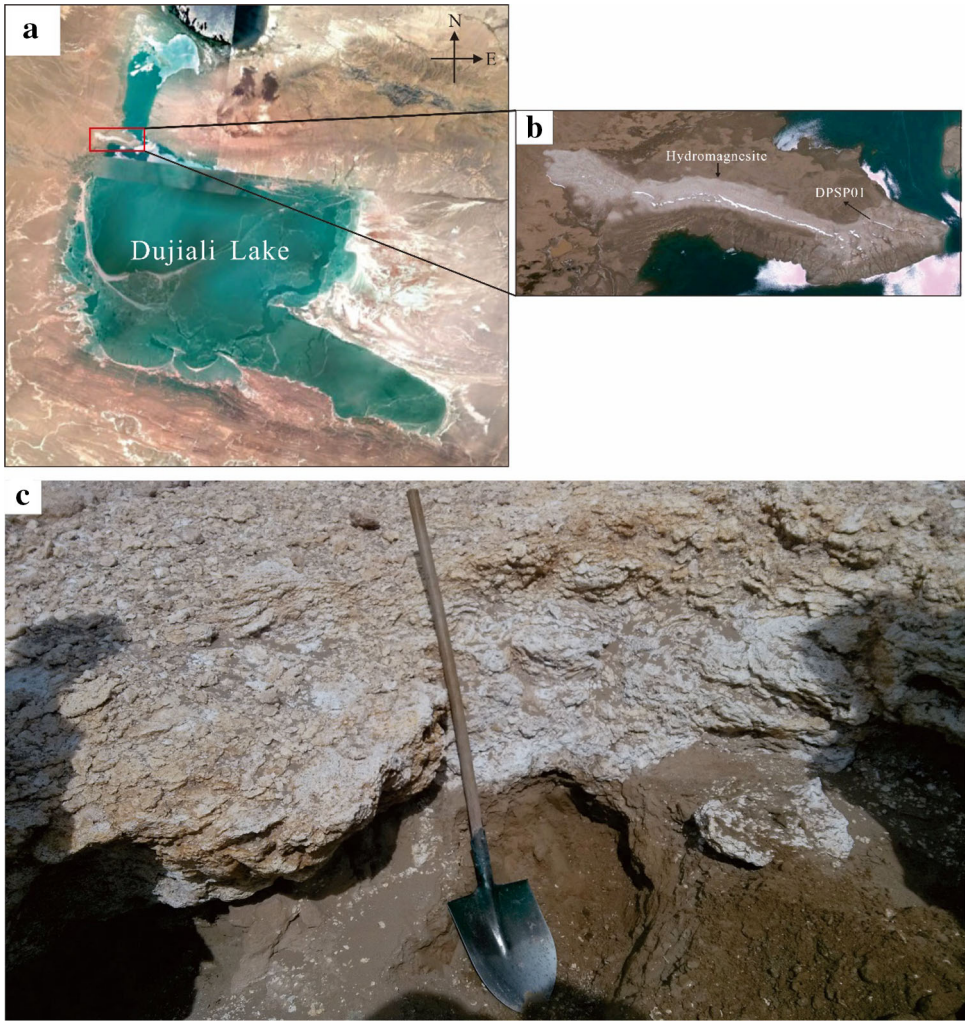

Fig. 2 **a**, **b** Satellite images showing the hydromagnesite deposit location at Dujiali Lake, central Qinghai–Tibetan Plateau, China. **c** Photograph showing hydromagnesite directly deposited on Quaternary sediments

Institute of Uranium Geology (Beijing, China), Chinese Ministry for Nuclear Industries. Fusion glasses were prepared by mixing the sample with lithium borate flux ($Li_2B_4O_7$) in the proportion 1:10. Pretreatment procedures were described by Yang et al. (2007). Analytical precision was better than 5% for repeated analyses of Chinese national standards GB/T 14506.14-2010 and GB/T 14506.28-2010. Loss on ignition (LOI) was determined by weighing samples before and after 1 h of heating at 1075 ± 25 °C.

Trace element and rare earth analyses

Trace elements and rare earth elements were determined using inductively coupled plasma mass spectrometry (ICP-MS) at the Beijing Research Institute of Uranium Geology (Beijing, China), Chinese Ministry for Nuclear Industries. Rhodium (Rh) was used as the internal standard. This ICP-MS offers very low detection limits, and its analytical precision was better than 5%. A powdered aliquot (50 mg) of each sample was dissolved in ultra-pure acids in four steps: (1) a mixture of 3 ml of HF with 1 ml of HNO_3 and 1 ml of $HClO_4$ (1:1 w/deionized H_2O) was added to the sample in capped Teflon bombs, ultrasonicated and then heated for 24 h to dissolve any silicates and salts; (2) re-dissolved in 3 ml of HNO_3 (1:1 w/deionized H_2O) in capped Teflon bombs for 7 days on a hot plate to further dissolve silicates, fluorides and zircons; (3) 3 ml of HNO_3 (1:1 w/deionized H_2O) was added to ensure complete dissolution of fluorides and dried on a hot plate; (4) samples were finally treated with 3 ml of HNO_3 (1:1 w/deionized H_2O), and at this stage no residue was observed. Solutions were transferred to clean flasks and were diluted with 1% HNO_3 to a total volume of 50 ml.

To determine the boron concentrations of the hydromagnesite samples, 50-mg aliquots of each powdered sample were digested in ultra-pure acids in three steps: (1) a mixture of 1 ml each of HNO_3, H_3PO_4, HCl, HF, and mannitol was added to each sample in capped Teflon bombs, ultrasonicated and then heated for 2 h; (2) samples were transferred to 50-ml quartz beakers containing 20 ml

of boiling deionized water, followed by addition of two drops of phenolphthalein with ammonia (1:1 w/deionized H_2O) neutralized to phenolphthalein red; (3) transferred into 50-ml quartz volumetric flasks, diluted with high-purity deionized water, and then immediately filtered into clean plastic bottles.

Scanning electron microscopy

Scanning electron microscopy (SEM) of hydromagnesite samples was performed at the Centre for High-Throughput Phenogenomics at The University of British Columbia. Samples were mounted onto aluminum stubs using 12-mm carbon adhesive tabs and coated iridium (10 nm) using a Leica EM MED020 coating system. Imaging was performed using an FEI Helios NanoLab 650 emission SEM, operating voltage of 1.0 kV, to produce high-resolution images.

Results

Mineralogy and crystal morphology

Based on XRD analysis, sediment samples were composed of pure hydromagnesite (Fig. 4). As observed using SEM, sediments comprised interlocking crystals of hydromagnesite (Fig. 3b). The hydromagnesite crystals were plate-like in morphology, submicron to several microns in width, and ~100 nm in thickness (Fig. 3c–e).

Major and trace elements composition

The major element compositions of the hydromagnesite samples are presented in Table 1. MgO and loss on ignition (LOI) were the dominant components, ranging from 40.85 to 42.78% (avg. = 41.66%, SD = 0.656) and 53.18 to 54.8% (avg. = 54.21%, SD = 0.656), respectively. Hydromagnesite with ideal stoichiometry has 43.1% MgO and 56.9% LOI ($H_2O + CO_2$). The CaO and Si content ranged from 1.33 to 2.85% (avg. = 1.83%, SD = 0.527) and 0.725 to 2.44% (avg. = 1.61%, SD = 0.634), respectively. The Al_2O_3, Fe_2O_3, Na_2O, K_2O, P_2O_5, TiO_2, FeO and MnO contents were all less than one percent (Table 1).

The data on 28 trace elements including redox-sensitive trace elements (Ni, Co, V, Cr, Th, U) are listed in Table 2. The most abundant trace element was Sr (avg. = 95.99 ppm), followed by Li, B, Ba (22.07, 20.73, 18.29 ppm average values, respectively). Element enrichment factors (EF_{UCC}) were used to compare hydromagnesite enrichments to upper continental crust (UCC; Taylor and McLennan 1985; Fig. 5). The trace elements in hydromagnesite are characterized as being significantly depleted relative to the UCC with the exception of Li and B.

REE compositions

Hydromagnesite REE + Y concentrations are presented in Table 3, and PAAS-normalized REE + Y patterns are shown in Fig. 6. Y is inserted between Dy and Ho in the REE pattern because of its identical charge and similar ionic radius (Bau and Dulski 1996). PAAS-normalized anomalies are calculated as a ratio between the measured and calculated concentration of a given element where the calculated concentration is determined either by a linear or geometric average of the nearest neighbor element concentration (Ge et al. 2010). The difference in the results obtained from these two methods is insignificant in most cases (<5%; Frimmel 2009). The Eu and Ce anomalies were determined, respectively, by $Ce/Ce^* = 2Ce_N/(La_N + Pr_N)$ and $Eu/Eu^* = 3Eu_N/(2Sm_N + Tb_N)$, while the Ce_{anom} are defined by $Ce_{anom} = \log(Ce/Ce^*)$. The Pr/Pr* anomaly is defined by $Pr/Pr^* = 2Pr_N/(Ce_N + Nd_N)$, (Kamber and Webb 2001), where N refers to concentration normalized to PAAS (McLennan, 1989). The results of these calculations are listed in Table 3.

The total rare earth element ($\sum$REE) contents of Dujiali Lake hydromagnesite were very low, varying from 0.625 to 3.11 ppm with an average of 1.75 ppm. The PAAS-normalized REE + Y patterns of all hydromagnesite samples were similar and had slight heavy REE (HREE) enrichments (Fig. 6). In general, the PAAS-normalized REE patterns of the hydromagnesite samples showed the following characteristics: (1) slight light REE depletion [$(Nd/Yb)_N = 0.51–0.81$, avg. = 0.59] except for one sample with a minor light REE enrichment [$(Nd/Yb)_N = 1.57$], (2) slight negative Ce anomaly, which is expressed by the Ce/Ce* ratio [Ce/Ce* = 0.78–0.96, avg. = 0.89], and (3) a consistently positive Eu anomaly expressed by the Eu/Eu* ratio [Eu/Eu* = 1.4–3.6, avg. = 2.39].

Diagenesis can affect Ce anomalies (McArthur and Walsh 1984; Peckmann et al. 2009; Shields and Stille 2001); however, this effect can be excluded if there is no correlation between La_N/Sm_N and the Ce anomaly where $La_N/Sm_N > 0.35$ (Bian et al. 2012; Khan et al. 2012). The Dujiali Lake hydromagnesite exhibited no such correlation suggesting that diagenetic changes in REE contents were negligible. In addition, diagenesis can cause a negative correlation between Ce/Ce* and Dy_N/Sm_N, and a positive correlation between Ce/Ce* and $\sum$REE (Shields and Stille 2001). Comparisons of Ce/Ce* with La_N/Sm_N, Dy_N/Sm_N, and $\sum$REE in the hydromagnesite samples show no correlation indicating that the samples preserved the original redox conditions of the sedimentary formational environment and that diagenesis had little effect on these samples.

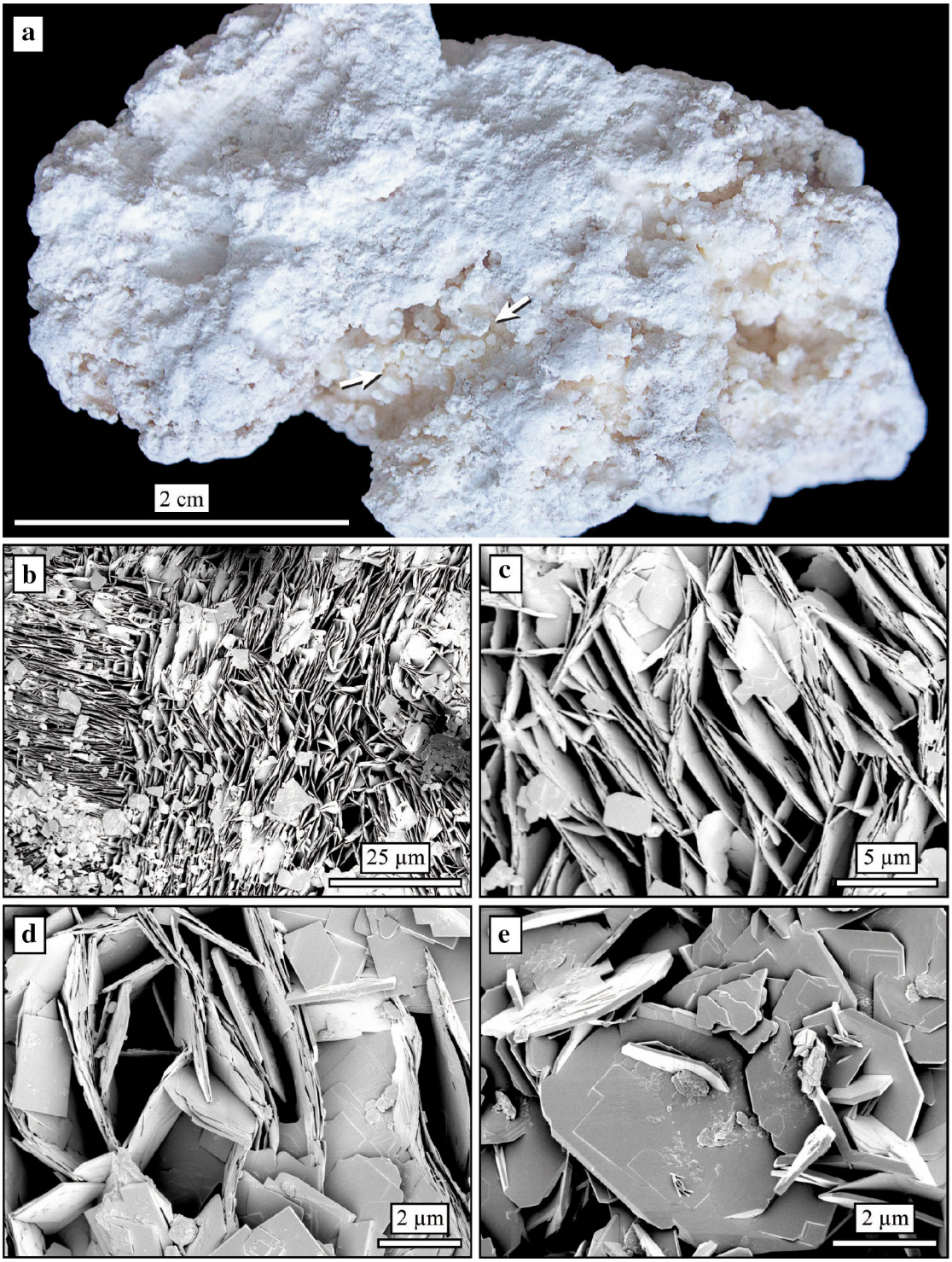

Fig. 3 **a** Photograph of a representative hand specimen of hydromagnesite showing cementation and globular texture (*arrows*). **b–e** Representative scanning electron micrographs showing interlocking platy hydromagnesite crystals

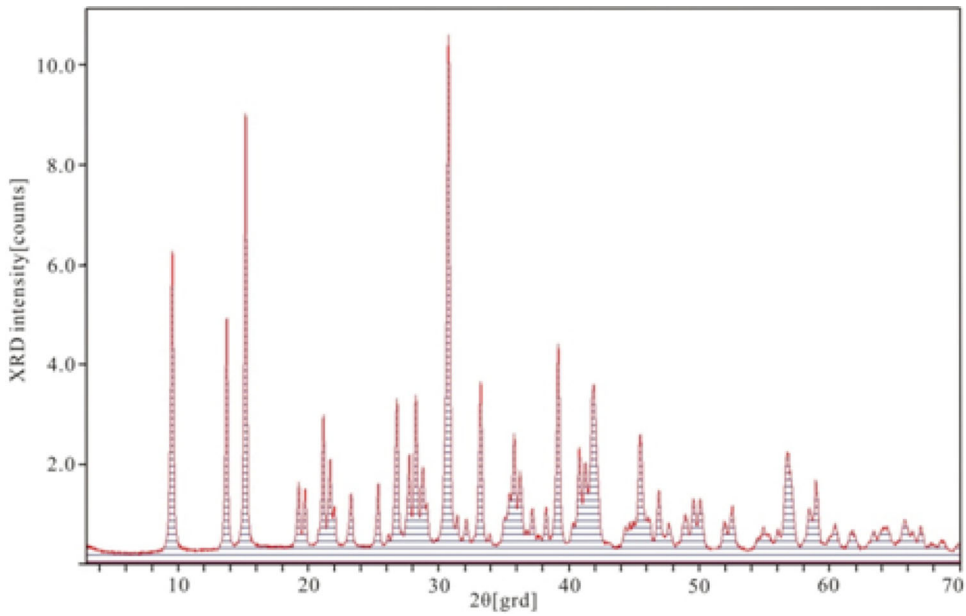

Fig. 4 Representative X-ray diffraction pattern of one of the hydromagnesite samples

Discussion

REE abundance patterns

Dujiali Lake hydromagnesite had low ∑REE values compared to typical marine carbonates (Sarkar et al. 2003); however, these data are consistent with hydromagnesite samples from Salda Gölü, Turkey (Zedef and Russell 2016). Furthermore, ∑REE values were similar to those reported for the Targejia hot spring cesium-rich geyserite deposits in Tibet, China (Zhao et al. 2007), travertine from Zhabuye Lake in Tibet, China (Zhao et al. 2010), and modern sinters from the geothermal waters on the Tibetan Plateau (Feng et al. 2014). Wright et al. (1987) showed that low REE concentrations in biogenic apatite from shallow water environments were attributed to fast sedimentation rates and burial that afford little time at the sediment–water interface. In addition, Ge et al. (2010) suggest that the low REE content of seep carbonate likely reflects a fast precipitation rate as there is limited time to incorporate REEs. Similarly, the low REE content of Dujiali Lake hydromagnesite may indicate a fast precipitation rate.

Europium anomaly

The Eu^{3+}/Eu^{2+} equilibria in aqueous solution are widely considered to be dependent on the pressure, pH, REE speciation, and most importantly, temperature based on the theoretical considerations and experimental results (Sverjensky 1984; Wood 1990; Bau and Möller 1992). At Earth's near-surface conditions, Eu^{3+} should predominate except possibly under very reducing, alkaline conditions, whereas Eu^{2+} will dominate at temperatures greater than about 250 °C (Sverjensky 1984). Consequently, europium in fluids will generally be divalent under most hydrothermal conditions (Sverjensky 1984). Nevertheless, significant

Table 1 Major element concentrations (%) for the Dujiali Lake hydromagnesite

Samples	SiO_2	Al_2O_3	Fe_2O_3	MnO	MgO	CaO	Na_2O	K_2O	TiO_2	P_2O_5	FeO	LOI
DJSP0101	2.44	0.427	0.055	<0.004	41.48	1.99	0.091	0.075	0.018	0.013	<0.10	53.18
DJSP0102	1.21	0.166	0.123	0.005	42.01	1.38	0.054	0.041	<0.006	0.01	<0.10	54.8
DJSP0103	2.28	0.628	0.153	0.006	40.97	2.04	0.085	0.069	0.017	0.016	0.13	53.72
DJSP0104	1.1	0.279	0.189	0.004	41.86	1.61	0.07	0.042	0.014	0.014	0.16	54.95
DJSP0105	1.6	0.319	0.218	0.004	40.85	2.85	0.01	0.058	0.016	0.013	0.18	53.9
DJSP0106	1.88	0.437	0.262	<0.004	41.65	1.6	0.033	0.065	0.013	0.021	0.23	54.2
DJSP0107	0.725	0.199	0.169	0.004	42.78	1.33	0.045	0.028	0.011	0.011	0.13	54.75

Table 2 Trace element concentrations (ppm) for the Dujiali Lake hydromagnesite

	DJSP0101	DJSP0102	DJSP0103	DJSP0104	DJSP0105	DJSP0106	DJSP0107
Ba	20.10	12.90	17.10	15.80	26.90	22.10	13.10
Co	0.48	0.32	0.45	0.29	0.43	0.35	0.24
Li	25.60	23.50	22.50	18.50	22.10	22.70	19.60
Ni	1.57	0.85	1.41	0.90	1.45	1.07	1.06
Pb	0.84	0.57	0.67	0.42	0.70	0.62	0.53
Zr	3.21	1.02	1.11	1.39	1.52	1.36	0.55
Sc	1.00	1.01	0.93	0.85	1.13	1.23	1.27
Hf	0.07	0.03	0.03	0.04	0.05	0.04	0.01
Rb	2.85	1.41	1.68	1.60	2.08	2.58	0.70
Sr	101.00	69.80	102.00	88.00	169.00	77.10	65.00
B	26.20	21.00	19.50	19.90	20.80	21.10	16.60
Be	0.04	0.03	0.02	0.03	0.01	0.04	0.03
Sc	1.00	1.01	0.93	0.85	1.13	1.23	1.27
V	2.32	1.38	1.35	1.31	1.12	1.30	0.85
Cr	2.29	1.17	1.37	1.48	1.45	1.60	1.65
Cu	1.07	0.57	0.60	0.49	0.65	0.50	0.68
Zn	1.36	0.78	1.20	0.55	1.86	1.62	4.52
Mo	0.15	0.05	0.04	0.03	0.02	0.04	0.12
Cd	0.02	0.01	0.01	0.00	0.01	0.00	0.00
Sb	0.13	0.07	0.09	0.07	0.05	0.03	0.87
Cs	0.81	0.19	0.26	0.23	0.23	0.28	0.09
Ba	20.10	12.90	17.10	15.80	26.90	22.10	13.10
Th	0.32	0.20	0.19	0.19	0.26	0.23	0.12
W	0.34	0.15	0.23	0.12	0.08	0.07	0.06
Bi	0.03	0.02	0.01	0.01	0.01	0.01	0.00
U	0.15	0.13	0.13	0.08	0.13	0.10	0.04
Nb	0.34	0.27	0.18	0.22	0.19	0.15	0.08
Ta	0.04	0.04	0.03	0.03	0.02	0.02	0.02

activities of Eu^{2+} and Eu^{3+} and their related complexes may occur in aqueous solutions at temperatures of approximately 100 °C depending on solution pH, oxidation state, and activities of ligands including carbonate (Sverjensky 1984).

Eu and Ce commonly behave differently compared to other REEs as they are more sensitive to changes in redox conditions (Leybourne et al. 2000). The occurrence of Eu and Ce anomalies in natural aqueous systems are due to the redox reactions that are shown in the following equations, where the reactants are thought to be indicative of reducing conditions and the products indicative of oxidizing conditions:

$$2Eu^{3+} + 2OH^{-} \rightarrow 2Eu^{2+} + H_2O + 0.5O_2 \quad (1)$$

$$2Ce^{3+} + 3H_2O + 0.5O_2 \rightarrow 2CeO_2 + 6H^{+} \quad (2)$$

Wood (1990) suggested that the Ce^{4+}/Ce^{3+} redox potential and Ce complex formation constants increase with increasing temperature and that the Ce^{4+}/Ce^{3+} redox equilibrium will also shift towards higher oxygen fugacity. The Dujiali Lake hydromagnesite samples show a slightly negative Ce anomaly and a consistently positive Eu anomaly. This combination of anomalies suggests changing redox conditions during hydrothermal fluid mixed with lake water from which the hydromagnesite precipitated.

Cerium anomaly

Cerium may be present in aqueous solutions as either trivalent (Ce^{3+}) or tetravalent species (Ce^{4+}). Ce^{3+} is more soluble than Ce^{4+} and is, therefore, less likely to be incorporated into precipitates. Thus, Ce depletion relative to neighboring rare earth elements can be explained by oxidation of Ce^{3+} to less soluble Ce^{4+} (Sholkovitz et al. 1994). For example, negative Ce anomalies in marine calcites occur because dissolved oxygen oxidizes soluble Ce^{3+} to insoluble Ce^{4+} (Sarkar et al. 2003). Conversely, calcite precipitating under reducing conditions displays normal or sometimes enriched Ce concentrations. Furthermore, negative Ce anomalies in ancient and modern

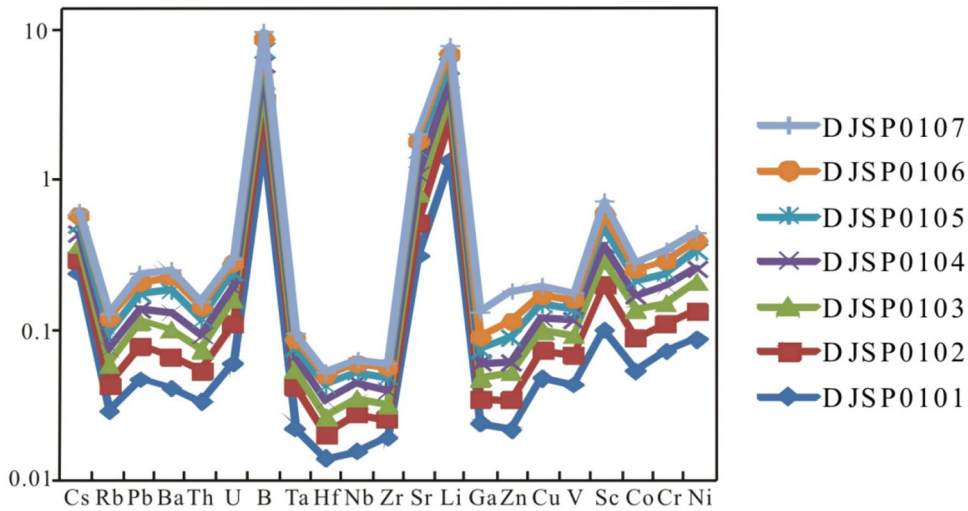

Fig. 5 Upper continental crust (UCC) normalized compositional distributions for Dujiali Lake hydromagnesite samples. Elements are listed in order of decreasing compatibility from *left* to *right*. UCC values are from Taylor and McLennan (1985)

Table 3 REE concentrations (ppm) for the Dujiali Lake hydromagnesite

	DJSP0101	DJSP0102	DJSP0103	DJSP0104	DJSP0105	DJSP0106	DJSP0107
La	0.61	0.33	0.32	0.24	0.37	0.6	0.13
Ce	1.17	0.58	0.57	0.45	0.59	1.15	0.24
Pr	0.14	0.07	0.07	0.05	0.08	0.13	0.03
Nd	0.66	0.26	0.29	0.2	0.28	0.55	0.12
Sm	0.13	0.06	0.05	0.05	0.05	0.09	0.02
Eu	0.03	0.01	0.01	0.01	0.01	0.02	0.01
Gd	0.08	0.05	0.04	0.03	0.05	0.06	0.02
Tb	0.02	0.01	0.01	0.01	0.01	0.01	0
Dy	0.09	0.03	0.06	0.05	0.07	0.07	0.02
Y	0.52	0.3	0.36	0.31	0.43	0.37	0.16
Ho	0.03	0.01	0.01	0.01	0.01	0.02	0
Er	0.05	0.03	0.03	0.03	0.04	0.03	0.02
Tm	0.01	0.01	0.01	0	0.01	0.01	0
Yb	0.09	0.04	0.04	0.02	0.05	0.03	0.02
Lu	0.01	0.01	0	0.01	0.01	0.01	0
∑REE	3.11	1.47	1.5	1.16	1.63	2.76	0.63
Nd_N/Yb_N	0.61	0.55	0.58	0.81	0.51	1.57	0.51
Ce/Ce*	0.92	0.9	0.87	0.92	0.78	0.96	0.92
log(Ce/Ce*)	−0.04	−0.05	−0.06	−0.04	−0.11	−0.02	−0.04
Eu/Eu*	2.35	1.41	2.04	3.13	1.83	2.39	3.56

seep carbonate minerals have been associated with temporary oxic conditions (Ge et al. 2010; Birgel et al. 2011; Wang et al. 2015). Therefore, a negative Ce anomaly has long been considered a sensitive indicator of oxidizing conditions (Liu et al. 1988; Kamber and Webb 2001; McArthur and Walsh 1984; Wright et al. 1987; Shields and Stille 2001; Sarkar et al. 2003; Tostevin et al. 2016).

The analysis of Ce/Ce* vs. Pr/Pr* recommended by Bau and Dulski (1996) can help evaluate whether the aberrant Ce/Ce* ratio results from anomalous La content or represents a real Ce anomaly. In the plot of Ce/Ce* versus Pr/Pr* (Fig. 7), almost all hydromagnesite samples lie in the area indicating no anomalies, except one sample that showed a slightly real negative Ce anomaly. Thus, the appearance of no real negative Ce suggests that reducing hydrothermal fluids influenced the waters from which the hydromagnesite precipitated, and that precipitation occurred rapidly.

Selected trace elements

Previous studies have demonstrated that some trace elements including Ni, Co, V, Cr, Th, and U are redox-sensitive elements in sediments (Goldschmidt 1954; Wignall

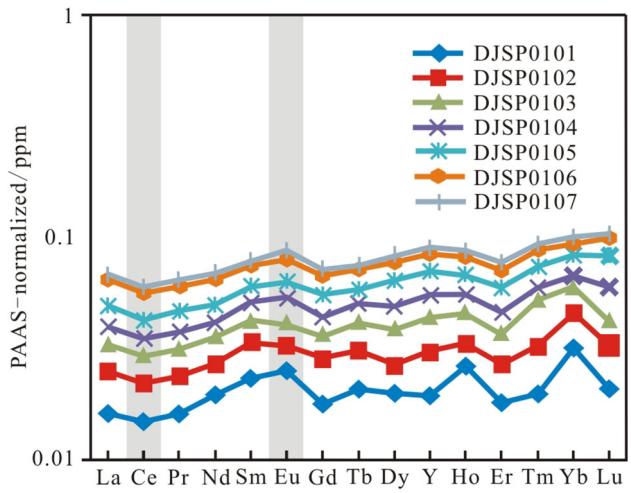

Fig. 6 Post-Archean Australian Shale (PAAS)-normalized REE patterns of Dujiali Lake hydromagnesite

and Myers 1988; Jones and Manning 1994; Algeo and Maynard 2004; Tribovillard et al. 2006; Manthilake et al. 2008; Johnson et al. 2010; Sáez et al. 2011). Tribovillard et al. (2006) state that there tends to be authigenic enrichments of redox-sensitive trace elements in oxygen-depleted sedimentary deposits because these elements are less soluble under reducing conditions compared to oxidizing conditions. Trace elements respond in predictable manner to varying redox conditions, and it is best to analyze a suite of trace elements rather than a single elemental proxy (Tribovillard et al. 2006). Jones and Manning (1994) suggest that Ni/Co ratios <5 infer oxic conditions, 5–7 dysoxic conditions, and >7 suboxic to anoxic conditions. The authors also used V/Cr ratios <2 to infer oxic conditions, 2–4.25 for dysoxic conditions and >4.25 for suboxic to anoxic conditions. Using this classification system, data from all hydromagnesite samples indicate formation under oxic conditions (Fig. 8). In addition, Hatch and Leventhal (1992) used V/V + Ni ratios to indicate redox conditions based on comparing to the degree of pyritization and other geochemical redox indicators. The authors propose that V/V + Ni ratios > 0.84 infer euxinic conditions, 0.54–0.82 for anoxic conditions and 0.46–0.60 for dysoxic conditions. Again, almost all the hydromagnesite samples plot within the oxic ranges delineated by Hatch and Leventhal (1992; Fig. 9).

Manganese has limited use as a proxy for redox conditions (Calvert and Pedersen 1993); however, it plays a prominent role in the transfer of trace elements from aqueous solution to sediments because of its peculiar geochemical behavior (Tribovillard et al. 2006). Mn oxides in sediments may trap metals, thereby preventing them from diffusing into overlying waters. These metals can return to the aqueous solution or be fixed in authigenic minerals depending on the sedimentary redox conditions (Tribovillard et al. 2006). Fe and Mn exhibit similar redox cycling, but Mn^{2+} and Fe^{2+} behave differently in terms of their oxidation kinetics (Calvert and Pedersen 1993, 1996). Under different redox conditions, Fe and Mn species form compounds with variable solubilities (Cullers 2002). For instance, Fe tends to be incorporated in sulfides under reducing conditions below the redox boundary, while Mn tends to accumulate in more oxygenated conditions above the redox boundary (Bellanca et al. 1996; Cullers 2002). Thus, Mn* values (Eq. 3) are a useful indicator of redox conditions for depositional environments (Machhour et al. 1994; Bellanca et al. 1996; Cullers 2002):

$$Mn* = \log\left[\left(Mn_{sample}/Mn_{shales}\right)/\left(Fe_{sample}/Fe_{shales}\right)\right] \quad (3)$$

The mean values of the Mn_{shales} and Fe_{shales} are reported by Wedepohl (1978). The hydromagnesite samples had slightly positive Mn* values suggesting the Dujiali Lake hydromagnesite was deposited under more oxidizing conditions.

Uranium is mobilized as U^{6+} under oxidizing conditions and precipitated as U^{4+} under reducing conditions (Wright et al. 1984). The U/Th ratio is a potential indicator of redox conditions because Th is relatively immobile in sedimentary environments and, therefore, concentrates in detritus (Wright et al. 1984; Martinez-Ruiz et al. 2000). Authigenic uranium, calculated as U_a = total U − Th/3, has also been used as an indicator of bottom-water oxygenation and is considered a reliable redox proxy (Wignall and Myers 1988; Jones and Manning 1994). Wignall and Myers (1988) suggested that oxic and dysoxic environments are separated by a U_a value of 2 ppm, whereas Jones and

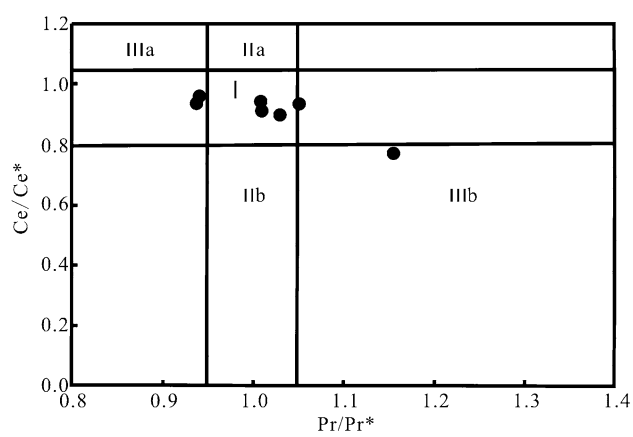

Fig. 7 Plot of Ce/Ce* vs. Pr/Pr* (after Bau and Dulski 1996). Field I: no anomalies; field IIa: positive La anomaly, no Ce anomaly; field IIb: negative La anomaly, no Ce anomaly; field IIIa: real positive Ce anomaly; field IIIb: real negative Ce anomaly. Most hydromagnesite samples showed no anomalies, except one with a slightly negative Ce anomaly

Manning (1994) used a U_a value of 5 ppm and a U/Th ratio of ~0.75 to distinguish these two conditions. The U/Th ratio in Dujiali Lake hydromagnesite was very low, varying from 0.36 to 0.66, with an average value of 0.51. The U_a content in the Dujiali Lake hydromagnesite varied from 0.004 to 0.064 ppm with an average value of 0.038 ppm. Accordingly, these data further demonstrate that the Dujiali Lake hydromagnesite formed in an oxidizing environment.

The Tibetan Plateau has at least 354 geothermally active areas based on incomplete statistics (Tong et al. 1981). The plateau's geothermal waters have higher Li concentrations in comparison to its rivers and springs, and are thus an important Li source (Zheng et al. 1995). When comparing the Li concentration of Dujiali Lake hydromagnesite with the seep, stream, and Dujiali Lake water (Lin et al. 2017), the hydromagnesite samples showed higher Li contents (avg. = 22.07 ppm). This finding suggests that geothermal or hydrothermal waters have influenced those that precipitated hydromagnesite.

Controls on hydromagnesite formation at Dujiali Lake

It is widely understood that the key processes that form authigenic carbonate minerals in lakes are (1) loss or extraction of CO_2 mainly by degassing, (2) evaporative concentration of solutes, and (3) mixing of different waters (Müller et al. 1972). In addition, the deposition of hydromagnesite in alkaline lake requires high Mg/Ca ratios and Mg concentrations. It has been suggested that Mg/Ca ratios of >39 are generally required for hydromagnesite formation in modern lacustrine microbialites (Chagas et al. 2016) and >50 in lacustrine carbonates (Last and Last 2012). For instance, Power et al. (2014) found that water discharging into hydromagnesite–magnesite playas in British

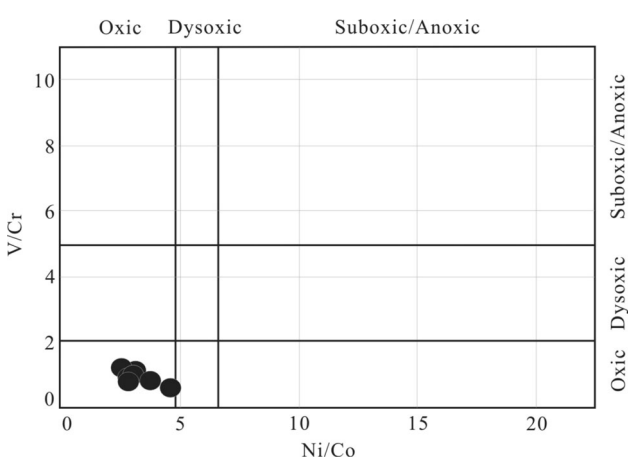

Fig. 8 Cross plots of redox-sensitive trace element ratios V/Cr vs. Ni/Co. Ranges for V/Cr and Ni/Co are from Jones and Manning (1994)

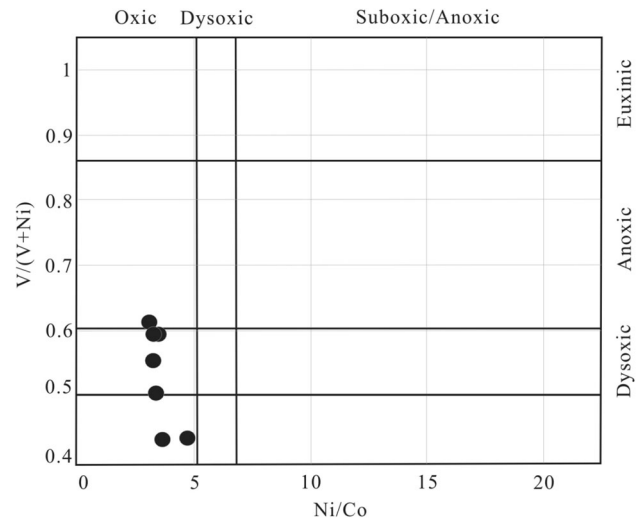

Fig. 9 Cross plots of redox-sensitive trace element ratios V/(V + Ni) vs. Ni/Co. Ranges for V/(V + Ni) are from Hatch and Leventhal (1992)

Columbia, Canada had a Mg/Ca ≈ 100, which may increase further after the precipitation of calcium carbonate minerals in the playas. In evaporation experiments of water from Tuz Gölü, Turkey, Müller et al. (1972) found that hydromagnesite was only precipitated when Mg/Ca ratios were >500 and Mg concentrations >34 g/L. In a study with particular relevance to the present one, Yu et al. (2015) carried out evaporation experiments using Dujiali Lake water, which showed that the precipitation sequence through natural evaporation in the field was first mirabilite followed by carbonate-containing alkaline salts [halite—NaCl, trona—$Na_2CO_3{\cdot}NaHCO_3{\cdot}2H_2O$, burkeite—$Na_6(CO_3)(SO_4)_2$, nahcolite—$NaHCO_3$, northupite—$Na_3Mg(CO_3)_2Cl$], and the finally boron- and potassium-bearing minerals. However, there was no Mg carbonate precipitation except for northupite [$Na_3Mg(CO_3)_2Cl$] in this experiment.

While the hydrogeochemistry of groundwater near Dujiali Lake has not been determined, it is likely that the main source is the Mg and dissolved inorganic carbon. The weathering of ultramafic rocks in the Banggong–Nujiang ophiolite mélange zone certainly produces Mg-rich groundwater. These Mg-rich waters likely discharge near or into Dujiali Lake, where CO_2 degassing and evaporation drive the precipitation of hydromagnesite. There are several examples of hydromagnesite deposits that result from ophiolite weathering including the hydromagnesite–magnesite playas in northern British Columbia, Canada (Power et al. 2014) and the hydromagnesite microbialites in Turkey (Braithwaite and Zedef 1996). Hydrated Mg carbonate minerals readily transform to less hydrated, more stable phases under Earth's surface conditions (Hopkinson et al. 2012; Königsberger et al. 1999; Power et al. 2016).

No evidence was gathered that would indicate Dujiali Lake hydromagnesite formed from a precursor, yet this possibility cannot be excluded.

With respect to the precipitation of hydromagnesite under predominantly oxic conditions, we propose a physicochemical model: alkaline Mg-rich groundwater flowed up to the near-surface or discharged at the surface of Dujiali Lake in the form of alkaline springs, and experienced either mixing with surface water or shallow water as well as air–water interaction. Air–water interaction allows the absorption of CO_2 directly from the atmosphere and results in the formation of hydromagnesite by evaporation. In our previous study at Dujiali Lake, we had proposed the supergene formation of authigenic hydromagnesite resulting from evaporation with atmospheric CO_2 being the major carbon source; thus, sequestering both natural and anthropogenic CO_2 (Lin et al. 2017). Our depositional model provides valuable insights for the interpretation of modern and ancient Mg carbonate deposits and the potential for harnessing of natural processes for sequestering atmospheric CO_2.

Conclusions

Trace and rare earth element geochemistry of hydromagnesite deposits in Dujiali Lake offer insights regarding the chemical and depositional environments of hydromagnesite formation. The total REE contents ($\sum$REE) of the hydromagnesite were low and had a narrow variation. Comparisons of Ce/Ce* with La_N/Sm_N, Dy_N/Sm_N, and $\sum$REE in the hydromagnesite samples showed no correlation indicating that the samples preserved the original redox conditions of the sedimentary formational environment. Redox-sensitive trace element ratios (U/Th, Ni/Co, V/Cr and V/V + Ni), negative Ce anomalies and Mn* values as well as low U_a indicated a predominantly oxidizing environment for hydromagnesite deposition. The hydromagnesite samples were consistently enriched in Eu, which is attributed to a local hydrothermal fluid input. Thus, the hydromagnesite likely precipitated from mixtures of emergent Mg-rich hydrothermal fluids mixed with near-surface waters similar to the lake water. New observations and detailed analyses of hydromagnesite sediments in Dujiali Lake provide an improved understanding of the modes of sediment deposition and chemical conditions at the time of deposition.

Acknowledgements The authors would like to thank Dr. Andong Chen for assistance with sample preparation, and Yanhui Zhang, Liangsheng Zhang, and Chenguang Xia for their help analyzing the major and trace elements. Special thanks to the anonymous reviewer whose insightful comments led to the improvement of our manuscript. This research was supported by Joint Funds of National Natural Science Foundation of China and the People's Government of Qinghai Province (Grant number: U1407207), National Natural Science Foundation of China (Grant number: 41603048), and Projects of China Geological Survey (Grant number: DD20160025).

References

Akhtar T, Shireen K, Bashir E, Nassem S (2009) Characteristics of ultramafic rocks and associated magnesite deposits, Nal Area, Khuzdar, Balochistan, Pakistan. J Geol Min Res 1:034–041

Algeo TJ, Maynard JB (2004) Trace-element behaviour and redox facies in core shales of Upper Pennsylvanian Kansas-type cyclothems. Chem Geol 206(3–4):289–318

Barrat JA, Boulègue J, Tiercelin JJ, Lesourd M (2000) Strontium isotopes and rare-earth element geochemistry of hydrothermal carbonate deposits from Lake Tanganyika, East Africa. Geochimica et Cosmochimica Acta 64(2):287–298

Bau M, Dulski P (1996) Distribution of yttrium and rare-earth elements in the Penge and Kuruman iron-formations, Transvaal Supergroup, South Africa. Precambrian Res 79(1–2):37–55

Bau M, Möller P (1992) Rare earth element fractionation in metamorphogenic hydrothermal calcite, magnesite and siderite. Mineral Petrol 45:231–246

Bellanca A, Claps M, Erba E, Masetti D, Neri R, Premoil Silva I, Venezia F (1996) Orbitally induced limestone/marlstone rhythms in the Albian–Cenomanian Cismon section (Venetian region, northern Italy): sedimentology, calcareous and siliceous plankton distribution, elemental and isotope geochemistry. Palaeogeogr Palaeoclimatol Palaeoecol 126(3–4):227–260

Bian YY, Lin ZJ, Feng D, Chen DF (2012) Rare earth elements of seep carbonates and using them to trace redox variation at seep sites. J Trop Oceanogr 31(5):37–44 **(in Chinese)**

Birgel D, Feng D, Roberts HH, Peckmann J (2011) Changing redox conditions at cold seeps as revealed by authigenic carbonates from Alaminos Canyon, Northern Gulf of Mexico. Chem Geol 285(1–4):82–96

Bonales LJ, Muñoz-Iglesias V, Santamaría-Pérez D, Caceres M, Fernandez-Remolar D, Prieto-Ballesteros O (2013) Quantitative Raman spectroscopy as a tool to study the kinetics and formation mechanism of carbonates. Spectrochim Acta Part A Mol Biomol Spectrosc 116:26–30

Braithwaite CJR, Zedef V (1994) Living hydromagnesite stromatolites from Turkey. Sediment Geol 92(1–2):1–5

Braithwaite CJR, Zedef V (1996) Hydromagnesite stromatolites, sediments in an alkaline lake, Salda Golü, Turkey. J Sediment Res 66(5):991–1002

Calvert SE, Pedersen TF (1993) Geochemistry of recent oxic and anoxic sediments: implications for the geological record. Mar Geol 113:67–88

Calvert SE, Pedersen TF (1996) Sedimentary geochemistry of manganese: implications for the environment of formation of manganiferous black shales. Econ Geol 91(1):36–47

Canaveras JC, Hoyos M, Sanchez-Moral S, Sanz-Rubio J, Bedoya J, Soler V, Groth I, Schumann L, Laiz L, Conzalez I, Saiz-Jimenez C (1999) Microbial communities associated with hydromagnesite and needle-fiber aragonite deposits in a karstic cave (Altamira, Northern Spain). Geomicrobiol J 16(1):9–25

Cangemi M, Censi P, Reimer A, D'Alessandro W, Hause-Reitner D, Madonia P, Oliveri Y, Pecoraino G, Reitner J (2016) Carbonate precipitation in the alkaline lake Specchio di Venere (Pantelleria Island, Italy) and the possible role of microbial mats. Appl Geochem 67:168–176

Chagas AAP, Webb GE, Burne RV, Southam G (2016) Modern lacustrine microbialites: towards a synthesis of aqueous and

carbonate geochemistry and mineralogy. Earth Sci Rev 162:338–363

Cullers RL (2002) Implications of elemental concentrations for provenance, redox conditions, and metamorphic studies of shales and limestones near Pueblo, CO, USA. Chem Geol 191:305–327

Debruyne D, Hulsbosch N, Muchez P (2016) Unraveling rare earth element signatures in hydrothermal carbonate minerals using a source–sink system. Ore Geol Rev 72(1):232–252

Ekambaram V, Brookins DG, Rosenberg PE, Emanuel KM (1986) Rare-earth element geochemistry of fluorite-carbonate deposits in western Montana, U.S.A. Chem Geol 54(3–4):319–331

Feng JL, Zhao ZH, Chen F, Hu HP (2014) Rare earth elements in sinters from the geothermal waters (hot springs) on the tibetan plateau, china. J Volcanol Geoth Res 287:1–11

Fischbeck R, Müller G (1971) Monohydrocalcite, hydromagnesite, nesquehonite, dolomite, aragonite, and calcite in speleothems of the Fränkische Schweiz, Western Germany. Contrib Miner Petrol 33:87–92

Franchi F, Hofmann A, Cavalazzi B, Wilson A, Barbieri R (2015) Differentiating marine vs hydrothermal processes in Devonian carbonate mounds using rare earth elements (Kess Kess mounds, Anti-Atlas, Morocco). Chem Geol 409:69–86

Frimmel HE (2009) Trace element distribution in Neoproterozoic carbonates as palaeoenvironmental indicator. Chem Geol 258(3–4):338–353

Ge L, Jiang SY, Swennen R, Yang T, Yang JH, Wu NY, Liu JA, Chen DH (2010) Chemical environment of cold seep carbonate formation on the northern continental slope of South China Sea: evidence from trace and rare earth element geochemistry. Mar Geol 277(1–4):21–30

German CR, Elderfield H (1990) Application of the Ce anomaly as a paleoredox indicator: the ground rules. Paleoceanography 5(5):823–833

Goldschmidt VM (1954) Geochemistry. Oxford Press, New York

Green DI, Young B (2006) Hydromagnesite and dypingite from the northern Pennine Orefield, northern England. Proc Yorks Geol Soc 56(2):151–154

Hatch JR, Leventhal JS (1992) Relationship between inferred redox potential of the depositional environment and geochemistry of the Upper Pennsylvanian (Missourian) stark shale member of the Dennis Limestone, Wabaunsee County, Kansas, USA. Chem Geol 99(1–3):65–82

Haurie L, Fernández AI, Velasco JI, Chimenos JM, Ticó-Grau JR, Espiell F (2005) Synthetic hydromagnesite as flame retardant. A study of the stearic coating process. Macromol Symp 221:165–174

Haurie L, Fernández AI, Velasco JI, Chimenos JP, Ticó-Grau JP, Espiell F (2006) Synthetic hydromagnesite as flame retardant. Evaluation of the flame behaviour in a polyethylene matrix. Polym Degrad Stab 91(5):989–994

Hecht L, Freiberger R, Gilg HA, Grundmann G, Kostitsyn YA (1999) Rare earth element and isotope (C, O, Sr) characteristics of hydrothermal carbonates: genetic implications for dolomite-hosted talc mineralization at Göpfersgrün (Fichtelgebirge, Germany). Chem Geol 155(1–2):115–130

Hill C, Forti P (1997) Cave minerals of the world, 2nd edn. National Speleological Society, Huntsville

Himmler T, Bach W, Bohrmann G, Peckmann J (2010) Rare earth elements in authigenic methane-seep carbonates as tracers for fluid composition during early diagenesis. Chem Geol 277(1–2):126–136

Hollingbery LA, Hull TR (2010) The thermal decomposition of huntite and hydromagnesite—a review. Thermochim Acta 509(1–2):1–11

Hopkinson L, Kristova P, Rutt K, Cressey G (2012) Phase transitions in the system $MgO–CO_2–H_2O$ during CO_2 degassing of Mg-bearing solutions. Geochim Cosmochim Acta 76:1–13

Janet CM, Viswanathan B, Viswanath RP, Varadarajan TK (2007) Characterization and photoluminescence properties of MgO microtubes synthesized from hydromagnesite flowers. J Phys Chem C 111(28):10267–10272

Johnson CL, Hudson SM, Rowe HD, Efendiyeva MA (2010) Geochemical constraints on the Palaeocene-Miocene evolution of eastern Azerbaijan, with implications for the South Caspian Basin and eastern Paratethys. Basin Res 22:733–750

Jones B, Manning DAC (1994) Comparison of geochemical indices used for the interpretation of palaeoredox conditions in ancient mudstones. Chem Geol 111(1–4):111–129

Kamber BS, Webb GE (2001) The geochemistry of late Archaean microbial carbonate: implications for ocean chemistry and continental erosion history. Geochim Cosmochim Acta 65:2509–2525

Kamber BS, Webb GE, Gallagher M (2014) The rare earth element signal in Archaean microbial carbonate: information on ocean redox and biogenicity. J Geol Soc 171:745–763

Kaźmierczak J, Altermann W, Kremer B, Kempe S, Eriksson PG (2009) Mass occurrence of benthic coccoid cyanobacteria and their role in the production of Neoarchean carbonates of South Africa. Precambr Res 173(1–4):79–92

Khan KF, Dar SA, Khan SA (2012) Rare earth element (REE) geochemistry of phosphorites of the Sonrai area of Paleoproterozoic Bijawar basin, Uttar Pradesh, India. J Rare Earths 30:507–514

Königsberger E, Königsberger L, Gamsjager H (1999) Low-temperature thermodynamic model for the system $Na_2CO_3–MgCO_3–CaCO_3–H_2O$. Geochim Cosmochim Acta 63(19–20):3105–3119

Last FM, Last WM (2012) Lacustrine carbonates of the northern Great Plains of Canada. Sediment Geol 277–278:1–31

Leybourne MI, Goodfellow WD, Boyle DR, Hall GM (2000) Rapid development of negative Ce anomalies in surface waters and contrasting REE patterns in groundwaters associated with Zn–Pb massive sulphide deposits. Appl Geochem 15(6):695–723

Li R, Jones B (2014) Evaluation of carbonate diagenesis: a comparative study of minor elements, trace elements, and rare-earth elements (REE + Y) between Pleistocene corals and matrices from Grand Cayman, British West Indies. Sediment Geol 314:31–46

Lin Y, Zheng M, Ye C (2017) Hydromagnesite precipitation in the Alkaline Lake Dujiali, central Qinghai-Tibetan Plateau: constraints on hydromagnesite precipitation from hydrochemistry and stable isotopes. Appl Geochem 78:139–148

Liu YG, Miah MRU, Schmitt RA (1988) Cerium: a chemical tracer for paleo-oceanic redox conditions. Geochim Cosmochim Acta 52(6):1361–1371

Loope GR, Kump LR, Arthur MA (2013) Shallow water redox conditions from the Permian-Triassic boundary microbialite: the rare earth element and iodine geochemistry of carbonates from Turkey and South China. Chem Geol 351:195–208

Machhour L, Philip J, Oudin JL (1994) Formation of laminate deposits in anaerobic—dysaerobic marine environments. Mar Geol 117:287–302

Manthilake MAGM, Sawada Y, Sakai S (2008) Genesis and evolution of Eppawala carbonatites, Sri Lanka. J Asian Earth Sci 32(1):66–75

Martinez-Ruiz F, Ortega-Huertas M, Palomo I (2000) Positive Eu anomaly development during diagenesis of the K/T boundary ejecta layer in the Agost section (SE Spain): implications for trace-element remobilization. Terra Nova 11(6):290–296

McArthur JM, Walsh JN (1984) Rare-earth geochemistry of phosphorites. Chem Geol 47(3–4):91–220

McLennan SM (1989) Rare earth elements in sedimentary rocks: influence of provenance and sedimentary processes. Rev Mineral Geochem 21:169–200

Müller G, Irion G, Förstner U (1972) Formation and diagenesis of inorganic Ca–Mg carbonates in the lacustrine environment. Sci Nat 59:158–164

Northup E, Kathleen H, Lavoie D (2001) Geomicrobiology of caves: a review. Geomicrobiol J 18(3):199–222

O'Neil JR, Barnes I (1971) C^{13} and O^{18} compositions in some freshwater carbonates associated with ultramafic rocks and serpentinites: western United States. Geochim Cosmochim Acta 35(7):687–697

Oskierski HC, Dlugogorski BZ, Jacobsen G (2013) Sequestration of atmospheric CO_2 in chrysotile mine tailings of the Woodsreef asbestos mine, Australia: quantitative mineralogy, isotopic fingerprinting and carbonation rates. Chem Geol 358:156–169

Oskierski HC, Dlugogorski BZ, Oliver TK, Jacobsen G (2016) Chemical and isotopic signatures of waters associated with the carbonation of ultramafic mine tailings, Woodsreef Asbestos Mine, Australia. Chem Geol 436:11–23

Pan GT, Wang LQ, Li RQ, Yuan SH, Ji WH, Yin FG, Zhang WP, Wang BD (2012) Tectonic evolution of the Qinghai-Tibet Plateau. J Asian Earth Sci 53:3–14

Peckmann J, Thiel V, Michaelis W, Clari P, Gaillard C, Martire L, Reitner J (2009) Cold seep deposits of Beauvoisin (Oxfordian; southeastern France) and Marmorito (Miocene; northern Italy): microbially induced authigenic carbonates. Biol J Lin Soc 98(1):181–186

Power IM, Wilson SA, Thom JM, Dipple GM, Southam G (2007) Biologically induced mineralization of dypingite by cyanobacteria from an alkaline wetland near Atlin, British Columbia, Canada. Geochem Trans 8:229–247

Power IM, Wilson SA, Thom JM, Dipple GM, Gabites JE, Southam G (2009) The hydromagnesite playas of Atlin, British Columbia, Canada: a biogeochemical model for CO_2 sequestration. Chem Geol 260(3–4):286–300

Power IM, Wilson SA, Harrison AL, Dipple GM, McCutcheon J, Southam G, Kenward PA (2014) A depositional model for hydromagnesite–magnesite playas near Atlin, British Columbia, Canada. Sedimentology 61(6):1701–1733

Power IM, Harrison AL, Dipple GM (2016) Accelerating mineral carbonation using carbonic anhydrase. Environ Sci Technol 50(5):2610–2618

Rao TR, Chohan VS (1995) Kinetics of thermal decomposition of hydromagnesite. Chem Eng Technol 18(5):359–363

Realinho V, Haurie L, Antunes M, Velasco JI (2014) Thermal stability and fire behaviour of flame retardant high density rigid foams based on hydromagnesite-filled polypropylene composites. Compos B Eng 58:553–558

Renaut RW, Long PR (1989) Sedimentology of the saline lakes of the Cariboo Plateau, Interior British Columbia, Canada. Sediment Geol 64(4):239–264

Sáez R, Moreno C, González F, Almodovar GR (2011) Black shales and massive sulfide deposits: causal or casual relationships? Insights from Rammelsberg, Tharsis, and Draa Sfar. Miner Depos 46(5):585–614

Sarkar A, Sarangi S, Ebihara M, Bhattacharya SK, Ray AK (2003) Carbonate geochemistry across the Eocene/Oligocene boundary of Kutch, western India: implications to oceanic O_2-poor condition and foraminiferal extinction. Chem Geol 201(3–4):281–293

Shi RD (2007) SHRIMP dating of the Bangong Lake SSZ-type ophiolite: constraints on the closure time of ocean in the Bangong Lake-Nujiang River, northwestern Tibet. Chin Sci Bull 52:936–941

Shi RD, Yang JS, Xu ZQ, Qi XX (2005) Recognition of MOR- and SSZ-type ophiolites in the Bangong Lake ophiolite mélange, western Tibet: evidence from two kinds of mantle peridotites. Acta Petrologica et Mineralogica 24: 397–408 **(in Chinese)**

Shields G, Stille P (2001) Diagenetic constraints on the use of cerium anomalies as palaeoseawater redox proxies: anisotopic and REE study of Cambrian phosphorites. Chem Geol 175(1–2):29–48

Sholkovitz ER, Landing WM, Lewis BL (1994) Ocean particle chemistry: the fractionation of rare earth elements between suspended particles and seawater. Geochim Cosmochim Acta 58:1567–1579

Sverjensky DA (1984) Europium redox equilibria in aqueous solution. Earth Planet Sci Lett 67(1):70–78

Taylor SR, McLennan SM (1985) The continental crust: its composition and evolution: an examination of the geochemical record preserved in sedimentary rocks. Blackwell Science, Oxford, pp 1–312

Tong W, Zhang MT, Zhang ZF (1981) Geothermics in Tibet. Science Press, Beijing, pp 1–170 **(in Chinese)**

Tostevin R, Shields GA, Tarbuck GM, He T, Clarkson MO, Wood RA (2016) Effective use of cerium anomalies as a redox proxy in carbonate-dominated marine settings. Chem Geol 438:146–162

Tribovillard N, Algeo TJ, Lyons T, Riboulleau A (2006) Trace metals as paleoredox and paleoproductivity proxies: an update. Chem Geol 232:12–32

Trolle-Wachmeister HG (1827) Svenska Vetenskapsakademien, Stockholm, Handlingar: 18.von Kobell, Wolfgang Xavier Franz (1835) Journal für praktische Chemie, Leipzig 4:80

Wang SH, Yan W, Chen Z, Zhang N (2014) Rare earth elements in cold seep carbonates from the southwestern Dongsha area, northern South China Sea. Mar Pet Geol 57:482–493

Wang SH, Magalhães VH, Pinheiro LM, Liu JL, Yan W (2015) Tracing the composition, fluid source and formation conditions of the methane-derived authigenic carbonates in the Gulf of Cadiz with rare earth elements and stable isotopes. Mar Pet Geol 68:192–205

Webb GE, Kamber BS (2000) Rare earth elements in Holocene reefal microbialites: a new shallow seawater proxy. Geochim Cosmochim Acta 64(9):1557–1565

Wedepohl KH (1978) Manganese: abundance in common sediments and sedimentary rocks. In: Wedepohl KH (ed) Handbook of geochemistry. Springer, Berlin, pp 1–17

Wignall PB, Myers KJ (1988) Interpreting benthic oxygen levels in mudrocks: a new approach. Geology 16:452–455

Wilson SA, Dipple GM, Power IM, Thom JM, Anderson RG, Raudsepp M, Gabites JE, Southam G (2009) Carbon dioxide fixation within mine wastes of ultramafic-hosted ore deposits: examples from the Clinton Creek and Cassiar chrysotile deposits, Canada. Econ Geol 104(1):95–112

Wilson SA, Harrison AL, Dipple GM, Power IM, Barker SLL, Mayer KU, Fallon SJ, Raudsepp M, Southam G (2014) Offsetting of CO_2 emissions by air capture in mine tailings at the Mount Keith Nickel Mine, Western Australia: rates, controls and prospects for carbon neutral mining. Int J Greenh Gas Control 25:121–140

Wood SA (1990) The aqueous geochemistry of the rare-earth elements and yttrium: 1. Review of available low-temperature data for inorganic complexes and the inorganic REE speciation of natural waters. Chem Geol 88:99–125

Wright J, Seymour RS, Shaw HF (1984) REE and Nd isotopes in conodont apatite: variations with geological age and depositional environment. Spec Pap Geol Soc Am 196:325–340

Wright J, Schrader H, Holser WT (1987) Paleoredox variations in ancient oceans recorded by rare earth elements in fossil apatite. Geochim Cosmochim Acta 51(3):631–644

Yan RE, Xia ZK (1987) Hydromagnesite and Late Pleistocene Environment in Datong Basin, Shanxi Province. Acta Scicentiarum Nat Univ Pekin 2:98–110 **(in Chinese)**

Yang XP, Zhu BQ, White PD (2007) Provenance of aeolian sediment in the Taklamakan Desert of western China, inferred from REE and major-elemental data. Quat Int 175(1):71–85

Yi HS, Lin JH, Zhao XX, Zhou KK, Li JP, Huang HG (2008) Geochemistry of rare earth elements and origin of positive europium anomaly in Miocene-Oligocene lacustrine carbonates from Tuotuohe basin of Tibetan plateau. Acta Sedimentol Sin 26:1–10 **(in Chinese)**

Yu JJ, Zheng MP, Wu Q, Wang YS, Nie Z, Bu LZ (2015) Natural evaporation and crystallization of Dujiali salt lake water in Tibet. Chem Ind Eng Process 34:4172–4178 **(in Chinese)**

Yutaka S, Keizo U, Nobuyasu M, Masanori K (1978) Thermal decomposition of hydromagnesite $4MgCO_3 \cdot Mg(OH)_2 \cdot 4H_2O$. J Inorg Nucl Chem 40(1–3):979–982

Zedef V, Russell M (2016) Rare earth element content of cryptocrystalline magnesites of Konya, Turkey. In: AIP conference proceedings, vol 1726, no 1. doi:10.1063/1.4945942

Zedef V, Russell MJ, Fallick AE, Hall AJ (2000) Genesis of vein stockwork and sedimentary magnesite and hydromagnesite deposits in the ultramafic terranes of southwestern Turkey: a stable isotope study. Econ Geol 95(2):131–134

Zhao YY, Nie FJ, Hou ZQ, Li ZQ, Zhao XT, Ma ZB (2007) Geochemistry of Targejia hot spring type cesium deposit in Tibet. Miner Depos 26:163–174 **(in Chinese)**

Zhao YY, Zheng YF, Chen F (2009) Trace element and strontium isotope constraints on sedimentary environment of Ediacaran carbonates in southern Anhui, South China. Chem Geol 265(3–4):345–362

Zhao YY, Cui YB, Zhao XT (2010) Geological and geochemical features and significance of travertine in travertine-island from Zhabuye salt lake, Tibet, China. Geol Bull China 29(1):124–141 **(in Chinese)**

Zheng MP (1997) An introduction to Saline Lakes on the Qinghai-Tibet Plateau. Springer, Dordrecht, pp 1–294

Zheng MP, Xiang J, Wei XJ (1989) Saline Lake on the Qinghai-Xizang (Tibet) Plateau. Science Press, Beijing, pp 1–431 **(in Chinese)**

Zheng XY, Zhang MG, Dong JH, Gao ZH, Xu C, Han ZM, Zhang BZ, Sun DP, Wang KJ (1995) Salt Lakes in Inner Mongolia. Science Press, Beijing, pp 196−218, 229−247 **(in Chinese)**

Zheng XY, Zhang MG, Xu X, Li BX (2002) Saline lakes of China. Science Press, Beijing, pp 49–51 **(in Chinese)**